

Where applicable, the authors confirm that the experiments described here conform with The Physiological Society ethical requirements.

## PC6

### A novel mechanism of sphingosine 1-phosphate signalling in regulation of L-type $\text{Ca}^{2+}$ channel activity in cardiac myocytes

E. Eroume A Egom, Y. Li, H. Musa and M. Lei

Division of Cardiovascular and Endocrine Sciences, University of Manchester, Manchester, UK

Sphingosine 1-phosphate (S1P) is bioactive lipid derived from metabolism of sphingomyelin that has been implicated in regulation of many cellular functions including ion channel activities (Hla, 2000; Pyne, 2000). To determine the effect of S1P on L-type calcium current ( $\text{I}_{\text{Ca,L}}$ ) at basal and  $\beta$ -adrenergic stimulation conditions and underlying intracellular signalling pathways in rat ventricular cardiac myocytes, Western blot, immunocytochemistry and voltage patch clamping were used. The results are presented as mean  $\pm$  SEM. Analysis was performed using the paired or un-paired Student's t test as appropriate and significance was accepted at  $p < 0.05$ . At basal condition, perfusion of S1P (100nM) had no significant effect on  $\text{I}_{\text{Ca,L}}$  ( $n=6$ ,  $p>0.05$ ). The effect of S1P on  $\text{I}_{\text{Ca,L}}$  was then studied in the presence of  $\beta$ -adrenergic stimulation by perfusion of 100 nM isoproterenol (ISO), a  $\beta$ -adrenergic receptor agonist.  $\text{I}_{\text{Ca,L}}$  was significantly enhanced in the presence of 100 nM ISO, the peak current density at 0 mV increased by  $83.27 \pm 2.8\%$  from  $-3.44 \pm 0.07$  at the basal condition to  $-20.57 \pm 0.76$  pA/pF in the presence of ISO ( $p < 0.01$ ,  $n = 7$ ). ISO had a significant positive effect on  $\text{I}_{\text{Ca,L}}$ . Additional 100 nM S1P significantly blunt effect of ISO on  $\text{I}_{\text{Ca,L}}$  (in the presence of ISO), the peak current density at 0 mV increased by  $68.99 \pm 3.4\%$  from  $-3.44 \pm 0.07$  to  $-11.1 \pm 1.80$  pA/pF ( $p < 0.01$ ,  $n = 7$ ). Our immunocytochemistry results also showed the co-localization between PAK1 (p21 activated kinase) - PP2A (protein phosphatase 2A) ( $n=25$ ,  $p<0.001$ ). Western blotting showed that the S1P1 receptor expressed in the cells whereas no visualization of S1P2 and S1P3 signals were observed. In conclusion, in rat ventricular myocytes, S1P does not affect the basal activity of L-type Ca channels but reversed the effect of the  $\beta$ -adrenergic agonist ISO on this channel. This effect is probably through PAK1-PP2A-mediated signalling pathway via S1P1 receptor.

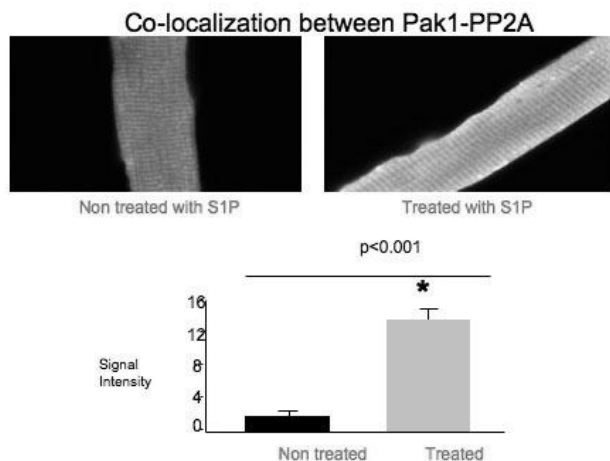


Figure 1.

Hla T, Lee MJ, Ancellin N, Thangada S, Liu CH, Kluk M, Chae SS, Wu MT (2000). *Ann N Y Acad Sci* 905, 16-24.

Pyne S, Pyne NJ (2000). *Biochem J* 349, 385-402.

This study was supported by the School of Medicine, University of Manchester and the Wellcome Trust. We thank Prof Mark Boyett group and Dr Jacqueline Ohanian for their support.

Where applicable, the authors confirm that the experiments described here conform with The Physiological Society ethical requirements.

## PC7

### Differential effects of ischemia and post-ischemia application of $\beta$ -adrenergic agonists in neonatal AV and SA nodal cells during reperfusion – a potential mechanism for Junctional Ectopic Tachycardia?

Y. Qu<sup>1,2</sup>, X. Sheng<sup>1,2</sup>, P. Dan<sup>1,2</sup>, E.A. Accili<sup>4</sup>, S. Sanatani<sup>3</sup> and G.F. Tibbitts<sup>1,2</sup>

<sup>1</sup>Child and Family Research Institute, Vancouver, BC, Canada, <sup>2</sup>Simon Fraser University, Burnaby, BC, Canada, <sup>3</sup>BC Children and Women's Hospital, Vancouver, BC, Canada and <sup>4</sup>University of British Columbia, Vancouver, BC, Canada

Cardiopulmonary bypass (CPB) is associated with an ischemia-reperfusion injury which can potentially impact the rhythmicity of the heart. Junctional Ectopic Tachycardia (JET) is the most common post-operative arrhythmia seen in neonates and infants undergoing CPB for repair of heart defects. Clinical evidence suggests JET originates from the AV node area and ischemia is speculated to be a pathogenic factor. JET is also associated with the post-operative administration of inotropes, in particular dopamine.

To determine how ischemia-reperfusion affects the pacemaker cell activity in neonates, AV nodal (AVNC) and SA nodal cells (SANC) were isolated from 10-day old New Zealand white rabbits and spontaneous action potentials were recorded using the perforated current clamp technique. Rabbits were anesthetized with thiopental sodium (60mg/kg) through intra-peritoneal injection prior to thoracotomy. The heart was rapidly excised and perfused with collagenase and subsequently protease in the Langendorff mode. AVNCs were dissociated from the AVN tissue cut at the triangle of Koch. SANCs were dissociated from the SAN tissue located adjacent to the crista terminalis. AVNCs and SANCs were identified by their automaticity, input resistance, and pacemaker current expression. We recorded APs during pre-ischemia, ischemia, post-ischemia with drugs and reperfusion with normal Tyrode's solution.

After 5 min exposure to the ischemia solution (pH 7.0, 5 mM lactate, 0 mM glucose), action potential (AP) frequency on AVNCs decreased and the AP duration was shortened ( $p < 0.05$ ,  $n=8$ , paired-samples t test); ischemia had no significant effect on SANCs over the same time period. Our results showed 20  $\mu\text{M}$  dopamine consistently led to irreversible irregular APs during reperfusion on AVNCs ( $n=4$ ) but not on SANCs. Typical changes in AP pattern were: slower upstroke, unstable maximal diastolic potentials, and an increase in early and delayed afterdepolarizations (EAD and DAD). Isoproterenol (1  $\mu\text{M}$ ) also induced AP

changes in AVNCs ( $n=3$ ) during reperfusion but to a lesser extent, without EAD but with DAD.

We conclude AVNCs are more susceptible to ischemia than SANs in neonates; we also demonstrate that the post-ischemia application of  $\beta$ -adrenergic agonists may exacerbate the trauma from ischemia and lead to irregular electrical activity in AVNCs during reperfusion. Whether JET results from a deterioration of AV conduction or abnormally enhanced AV automaticity needs to be explored further.

*Where applicable, the authors confirm that the experiments described here conform with The Physiological Society ethical requirements.*

## PC8

### Computational evaluation of the effects of novel anionic currents on human atrial electrical behaviour

S. Kharche<sup>1</sup>, J. Stott<sup>1</sup>, P. Law<sup>1</sup>, H. Zhang<sup>1</sup> and J.C. Hancox<sup>2</sup>

<sup>1</sup>School of Physics and Astronomy, University of Manchester, Manchester, Lancashire, UK and <sup>2</sup>Department of Physiology, Bristol Heart Institute, Bristol, UK

A novel outwardly rectifying anionic background current ( $I_{AN-ION}$ ) with small conductance ( $\leq 0.4$  pS/pF) has been recently identified in human atrium [1], which can contribute to shortening of atrial action potential duration (APD) during phase 2 repolarisation period. In this study, we computationally evaluated the functional effects of  $I_{AN-ION}$  on atrial electrical excitation-wave propagation and conduction in humans.

The cellular model of human atrial action potentials (APs) by Courtemanche *et al.* [2] was modified to incorporate  $I_{AN-ION}$  with either nitrate or chloride ( $NO_3^-$  or  $Cl^-$ ) ions as charge carriers [1]. The model was used to investigate the effects of the anionic background current on effective refractory period (ERP), and AP and ERP restitution. The single cell model was then incorporated into a homogenous multicellular model of human atrial tissue we developed in a previous study [3] to investigate the effects of the anionic current on intra-atrial conduction velocity restitution, tissue's vulnerability to re-entry and characteristics of re-entrant excitation waves, such as the frequency, lifespan and tip meandering pattern of re-entry.

Previous work has shown that inclusion of  $I_{AN-ION(Cl)}$  or  $I_{AN-ION(NO_3)}$  in the Courtemanche *et al.* model had only a minor ( $\sim 1$  mV) effect on atrial resting membrane potential and at an AP frequency of 1 Hz  $I_{AN-ION}$  abbreviated atrial APD<sub>50</sub> by  $\sim 10\%$  with  $Cl^-$  and  $\sim 13.5\%$  with  $NO_3^-$  as charge carrier without abbreviation of APD<sub>90</sub> [1]. The present simulations showed that, paradoxically, incorporation of  $I_{AN-ION}$  prolonged atrial ERP at a pacing cycle length of 1000 ms and flattened APD<sub>90</sub> restitution curve.  $I_{AN-ION}$  facilitated atrial conduction manifested by an increase in conduction velocity.  $I_{AN-ION}$  also increased atrial tissue vulnerability to genesis of re-entry (by 8.7 % for  $I_{AN-ION(Cl)}$  and 8.4 % for  $I_{AN-ION(NO_3)}$ ) in response to a premature stimulus applied to the refractory tails of a conditioning wave, because of facilitated inter-atrial conduction. Tip meandering pattern of re-entrant excitation waves was unaffected, decreased the frequency of electrical excitations, and increased the lifespan of the re-entry. Our simulations show that the outwardly rectifying anionic background current  $I_{AN-ION}$ , though small, nevertheless influences

atrial electrical AP morphology, APD, ERP and their rate dependencies. It affects intra-atrial conduction, tissue's vulnerability to genesis of re-entry and dynamic behaviours of re-entrant excitation waves.

Li H, Zhang H, Hancox JC, Kozłowski RZ (2007). *Biochem Biophys Res Commun* 359, 765-70.

Courtemanche M, Ramirez RJ & Nattel S (1998). *Am J Physiol* 275, H301-H321.

Kharche S, Seemann G, Leng J, Holden A.V., Garatt C J, Zhang H (2007). *LNCS* 4466, 129-138.

Biktasheva IV, Biktashev VN & Holden AV (2005). *LNCS* 3504, 293-303.

This work was supported by BHF (140/PG/03).

*Where applicable, the authors confirm that the experiments described here conform with The Physiological Society ethical requirements.*

## PC9

### Reduced conduction velocity caused by class Ib anti-arrhythmic drugs contributes to both their anti- and pro-arrhythmic effects in human virtual ventricular tissues

J.A. Lawrenson<sup>1</sup>, A.P. Benson<sup>2</sup> and A.V. Holden<sup>2</sup>

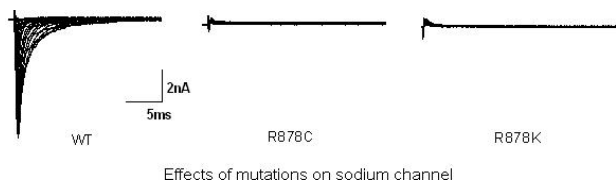
<sup>1</sup>School of Medicine, University of Leeds, Leeds, UK and <sup>2</sup>Institute of Membrane and Systems Biology, University of Leeds, Leeds, UK

Ventricular tachycardia and fibrillation are dangerous cardiac arrhythmias. Anti-arrhythmic drugs such as lidocaine (a class Ib drug) can prevent such arrhythmias, but they have pro-arrhythmic side effects whose mechanisms are poorly understood. We used computational models to elucidate these mechanisms.

Effects of lidocaine were simulated (1) in human ventricular cell models (2). The drug binds to the inactivated state of the sodium channel and has on and off rate constants of 31.0 /mM/s and 0.79 /s respectively, as measured experimentally in human ventricular cells (3). These drug effects were incorporated into 75 mm one-dimensional (1-D) heterogeneous transmural, and 12x12 cm two-dimensional (2-D) epicardial, virtual tissues (4). Drug effects were characterised and validated in single cell models. Simulated application of 0.08 mM lidocaine produced rate-dependent steady state (end systolic) block of the sodium current  $I_{Na}$  and reductions in maximum action potential upstroke velocity  $dV/dt_{max}$  (Table 1). There was little effect on action potential duration (APD). This is consistent with (5). In 1-D tissues, the reduced upstroke velocity under drug conditions caused reduced conduction velocity, and propagation block at short cycle lengths (CLs). The reduced conduction velocity was associated with an increased vulnerable window for unidirectional propagation (4). The maximum temporal width of the vulnerable window, expressed as a percentage of the diastolic interval, increased with pacing rate and simulated drug concentration, from 1% at CL = 1000 ms with 0.015 mM lidocaine to 18% at CL = 500 ms with 0.2 mM lidocaine. In 2-D virtual tissues, this reduced conduction velocity prevented initiation of re-entry (tachycardia), prevented breakdown of re-entry into fibrillation, or shortened the lifetime of re-entry, depending on simulated drug concentration.

We conclude that the anti-arrhythmic mechanism of class Ib drugs in the virtual tissues is reduced conduction velocity, and

R878C cells (n=20) did not show any detectable current. There was also no detectable current of R878K (n=10) with lysine substituting arginine at amino acid 878, demonstrating that the positive change at 878 is not the only key defect for the mutant channel. Further immunocytochemical characterization revealed that mutant channel had normal trafficking to the plasma membrane, which suggested that the mutant channel produced a non-functional channel phenotype but had normal intracellular trafficking to the plasma membrane.



Benson DW, Wang DW, Dymont M, Knilans TK, Fish FA, Strieper MJ, Rhodes TH & George AL, Jr (2003). *J Clin Invest* 112, 1019-1028.

Modell SM & Lehmann MH. (2006). *Genet Med* 8, 143-155.

Shimizu W. (2005). *Intern Med* 44, 1224-1231.

Wolf CM & Berul CI. (2006). *J Cardiovasc Electrophysiol* 17, 446-455.

This work is funded by The Wellcome Trust and Dorothy Hodgkin Postgraduate Award

*Where applicable, the authors confirm that the experiments described here conform with The Physiological Society ethical requirements.*

In both species, extensive areas of histologically discrete myocardium are found in the vestibules of the tricuspid and mitral valves. The areas are more extensive in guinea-pig than rat, and show the immunohistochemical characteristics of pacemaker tissue. The best developed part of these specialised tissues, apart from the AV conduction axis itself, is found in the atrial septum immediately posterior to the aortic root, an area previously described as the retroaortic knot (RAK). Immunofluorescence and confocal microscopy revealed that, as with the AV conduction axis of the heart, this RAK tissue is positive for the major isoform of the funny channel, HCN4, and negative for the major gap junction channel, Cx43. In addition, the RAK tissue, like other cardiac myocytes, expresses caveolin3, a membrane bound protein. We used the expression of caveolin3 to measure the diameter of RAK cells. The RAK cells are significantly larger than AV node cells, but significantly smaller than atrial and ventricular cells ( $10.34 \pm 0.99$ ,  $6.76 \pm 0.38$ ,  $14.45 \pm 0.61$  and  $18.92 \pm 0.58$   $\mu\text{m}$ , respectively). In both species, the RAK is in continuity with the rings of specialised myocytes that encircle the orifices of the tricuspid and mitral valves. We conclude that the ring tissues, including the RAK, expressing HCN4, may be capable of initiating spontaneous pacemaker activity, and could be a source of arrhythmias.

Kent AFS (1893). *J Physiol* 14, i2-254.

*Where applicable, the authors confirm that the experiments described here conform with The Physiological Society ethical requirements.*

## PC14

### In rat and guinea-pig hearts, the retroaortic knot expresses the major isoform of the funny channel - HCN4

J.F. Yanni<sup>1</sup>, M.R. Boyett<sup>1</sup>, R.H. Anderson<sup>2</sup> and H. Dobrzynski<sup>1</sup>

<sup>1</sup>Cardiac electrophysiology unit, Manchester University, Manchester, UK and <sup>2</sup>Cardiac Unit, Institute of Child Health, University College London, London, UK

It is well established that the atrioventricular (AV) conduction axis is the so-called "specialised" component of the junctions between the atrial and ventricular myocardial tissues, and that the bundle of His is the only muscular structure that, in the normal heart, crosses the plane of AV electrical insulation. It has remained controversial, however, as to whether other parts of the atrial vestibules are histologically specialised. Kent, in 1893, proposed that multiple muscular bridges cross from atrium to ventricle as the substrate for normal AV conduction. It is certainly the case that, in human hearts, remnants of histologically specialised myocardium are to be found on the atrial side of the insulating plane, albeit *without* making muscular connections with the ventricular myocardium, but the full extent of these so-called AV ring tissues has still to be established.

In the present study, using histology and immunoconfocal microscopy, we have investigated the specialised components of the AV junction in the hearts of four rats and guinea-pigs. The animals were humanely killed, and the hearts rapidly removed and frozen in liquid nitrogen. 20  $\mu\text{m}$  serial sections were then cut through the entirety of the AV junctions.

## PC15

### A novel model of heart rate variability based on ion channel kinetics in the sinoatrial node

M. Nirmalan<sup>1</sup> and M. Niranjan<sup>2</sup>

<sup>1</sup>Intensive Care Unit, Manchester Royal Infirmary, Manchester, UK and <sup>2</sup>Department of Computer Sciences, University of Sheffield, Sheffield, UK

Rate of spontaneous depolarization in the sino-atrial node (SAN) is modulated by sympathetic and parasympathetic neural inputs. These interactions manifest as variations in instantaneous heart rate, commonly referred to as heart rate variability (HRV). Mathematical models of HRV should therefore be based on effects of the autonomic nervous system on ion channel kinetics responsible for SAN automaticity. We describe a model of HRV based on the above interactions.

Generation of pace maker potential was simulated using an 'integrate and fire' model, analogous to the charging of a capacitor via a resistor, starting from a resting membrane potential (RMP) of -50 mV to a reversal potential of -15 mV. When the potential reaches a threshold of -40 mV, the action potential is triggered. Two specific enhancements were made to the above basic model. Firstly, Phase 4 depolarization was assumed to occur in two stages: an initial slow exponential rise followed by a second accelerated exponential rise [associated with voltage independent late diastolic spontaneous  $\text{Ca}^{2+}$  release (1)]. Secondly, time constants for membrane depolarization at successive epochs were the product of linear interactions between (a) inherent stochasticity in channel activity and (b) sinusoidal inputs from the sympathetic

(0.1Hz) and parasympathetic (0.25Hz) efferents that increased and decreased the open probability of ion channels respectively. Average heart-rate (beats per minute) and variability (standard deviation as a percentage of mean heart rate) at varying levels of input from the sympathetic and parasympathetic systems are shown in Table 1. Maximal variability was seen when depolarization occurred under both sympathetic and parasympathetic control (SD=34%). Variability was considerably lower when only one of the autonomic components was active (17%) and lowest when the heart was completely isolated from the autonomic inputs (0.1%).

We provide the first comprehensive model of HRV based on interactions between SAN ion channels and autonomic nerves. This model acknowledges two well recognized but, hitherto unexplained, features of HRV: namely (1) Low levels of HRV can be demonstrated in the absence of autonomic inputs (e.g isolated heart preparations); and (2) HRV is reduced during both sympathetic blockade (2) and sympathetic stimulation (3).

Sympathetic input	Parasympathetic input	Mean heart rate (bpm)	Variability SD as % of mean
0.0	0.0	60.0	0.13
0.0	1.0	43.4	16.7
1.0	0.0	89.0	17.4
1.0	1.0	61.0	33.9

Average heart rate and variability (SD of heart rate as a % of mean heart rate), under varying conditions of autonomic control

Vinogradova TM et al. (2004). *Circulation Research* 94, 802-809.

Lampert R et al. (2003). *American Journal of Cardiology* 91, 137-142.

Godin PJ et al. (1996). *Critical Care Medicine* 24, 1117-1124.

*Where applicable, the authors confirm that the experiments described here conform with The Physiological Society ethical requirements.*

## PC16

### Comparative physiology of the sinoatrial pacemaker of cold-blooded vertebrates

V.A. Golovko

*Institute of Physiology, Komi Science Centre, Urals Branch, Russian Academy of Sciences, Syktyvkar, Russian Federation*

It is known that the proximal and distal ends of the tubular heart of tunicates have two centres of automatism that work alternately. As a result, the blood advances by peristaltic contracting waves. Active animal living has led to the appearance of a bent tube with various chambers and valves between them. The pacemaker's cytoarchitecture also has changed. The aim of our study was to analyse the main parameters of the action potential (AP) in true pacemaker cells in the hearts of different poikilotherm species, including inhabitants of water (ammocoete, *Lampetra fluviatilis*, dace, *Leuciscus rutilus*) and land (frog, *Rana temporaria*, tortoise, *Testudo horsfieldi*). Experiments were carried out on spontaneously beating strips of sinoatrial (SA) tissue (control conditions: 20°C, 0.9 mM  $\text{Ca}^{2+}$ ), using the standard micro-electrode technique. In cold-blooded animals, in the evolutionary scale from Cyclostomata to Reptiles, true pacemaker cells are located along the full border between the sinus venosus and atrium. Two SA valves originated at this site and formed a roller

called 'the sinoatrial ring'. These modifications changed the working regime of the vertebrate's electromechanical pump from a peristaltic one to an impulse one. When the isolated SA ring of the dace's heart was divided into two, the frequency of AP generation in the left and right segments was  $69 \pm 11 \text{ min}^{-1}$ , ( $n=11$  strips) and  $72 \pm 9 \text{ min}^{-1}$  ( $n=11$ ,  $p>0.05$ ), respectively. However, the frequency of AP generation was higher ( $91 \pm 12 \text{ min}^{-1}$ ,  $p<0.05$ ) in the non-divided isolated dace's SA ring. The action potential duration at 90% repolarization ( $\text{APD}_{90}$ ) increased from the ammocoete ( $0.11 \pm 0.02 \text{ s}$ ,  $n=39$  cells) to the tortoise ( $1.1 \pm 0.15 \text{ s}$ ,  $n=72$ ). The rate of change of membrane potential ( $dV/dt$ ) during phase 3 was highest in the ammocoete ( $1.2 \text{ V s}^{-1}$ ) and lowest in the tortoise ( $0.2 \text{ V s}^{-1}$ ). Interestingly, the SA pacemaker of different animal species appeared to be heterogeneous in its resistance to  $\text{Ca}^{2+}$ -free solution. In particular, the ammocoete's heart continued generating APs for longer than 10 hours in  $\text{Ca}^{2+}$ -free solution, while complete blockade of AP generation was observed in strips of the tortoise heart after 5 min of perfusion with 0.45 mM  $\text{Ca}^{2+}$  solution. We propose that many of the  $\text{Ca}^{2+}$ -dependent mechanisms of pacemaker function can be found even in more genetically primitive creatures such as Metazoa.

*Where applicable, the authors confirm that the experiments described here conform with The Physiological Society ethical requirements.*

## PC17

### Gi2 plays a critical role in the short-term modulation of heart rate dynamics

Z. Zuberi<sup>1</sup>, L. Birnbaumer<sup>2</sup> and A. Tinker<sup>1</sup>

<sup>1</sup>Medicine, UCL, London, UK and <sup>2</sup>National Institute of Environmental Health Sciences, Research Triangle, NC, USA

Acetylcholine released from the vagus nerve acts on cardiac M2 receptors to cause negative chronotropic responses and this is due, in part to an increase in  $\text{K}^{+}$  conductance mediated by G-protein inwardly rectifying potassium (GIRK) channels (Sakmann et al. 1983). This process is pertussis toxin sensitive implicating  $\text{Gi/o}$  in GIRK channel activation. Ablation of cardiac GIRK channels at a molecular level leads to impaired parasympathetic responses in vivo (Wickman et al. 1994).  $\text{Gi}\alpha 2$  is considered the most abundant cardiac isoform. We screened mice on an Sv129 background with global genetic deletions of  $\text{Gi}\alpha 2$  and  $\text{Gi}\alpha 1$  and 3 as a double knockout with littermate controls (adjusted for age, weight and sex) and assessed negative chronotropic responses to intraperitoneal carbachol administration (500ng/g) under inhalation isoflurane anaesthesia. Maximal relative inhibitory response was attenuated in  $\text{Gi}\alpha 2$ -deficient mice (mean inhibition  $0.1152 \pm 0.024$ ,  $n=6$ ) compared to control ( $0.3261 \pm 0.054$ ,  $n=6$ ) or  $\text{Gi}\alpha 1/3$  ( $0.3280 \pm 0.080$ ,  $n=6$ ). Additionally, using heart rate variability analysis (HRV) of ECG data collected from implantable telemetry devices we were able to measure heart rate dynamics in conscious freely moving mice (Gehrmann et al. 2000). Our results suggest differential heart rate responses with respect to particular  $\text{Gi}\alpha$  isoform. Mean heart rate (HR) over 48hrs demonstrated that  $\text{Gi}\alpha 2$  (-/-) deficient mice had significantly higher nocturnal HR ( $\text{Gi}\alpha 2$ ,  $617.6 \pm 11.89$  ( $n=5$ ) vs control,  $568.5 \pm 14.64$  ( $n=6$ ) vs  $\text{Gi}\alpha 1/3$ ,  $579 \pm 8.2$  ( $n=6$ ) (1-way



Where applicable, the authors confirm that the experiments described here conform with The Physiological Society ethical requirements.

## PC31

### Propagation of the action potential through a 3D model of the rabbit right atrium including the conduction system

J. Li<sup>1</sup>, J.E. Schneider<sup>2</sup>, I.D. Green<sup>1</sup>, H. Dobrzynski<sup>1</sup> and M.R. Boyett<sup>1</sup>

<sup>1</sup>University of Manchester, Manchester, UK and <sup>2</sup>University of Oxford, Oxford, UK

Accurate simulation of the generation and propagation of cardiac electrical activity requires detailed electrophysiological and anatomical models. We have previously generated three-dimensional (3D) anatomical models of the sinoatrial node and the atrioventricular node (Dobrzynski et al., 2005; Li et al, 2004). The purpose of this study was to construct a 3D anatomical model of the rabbit right atrium with multiple objects, including the conduction system, and use this to simulate the propagation of the action potential through the right atrium. In this work, we used multiple techniques to generate the 3D anatomical model. The model was based on ~1500 images of the rabbit heart (atria and part of ventricles) obtained by high-resolution magnetic resonance imaging (MRI). MATLAB was used to analyse the data and generate a 3D anatomical model of the right atrium. The ~1500 two-dimensional images were stacked to produce a 3D array. Segmentation was carried out semi-manually by analysing the data using custom written programs developed in MATLAB. The sinoatrial node (SAN) and atrioventricular node (AVN) could be detected (and then segmented) after comparison of images with our existing models of the SAN and AVN. A 3D right atrium array model, including thirteen objects, was constructed. The objects are the right atrium, the SAN, the AVN, part of the right ventricle, the aorta with the aortic valve, the superior vena cava, the inferior vena cava, the coronary sinus, the tricuspid valve, part of the mitral valve, the fossa ovalis, the central fibrous body and outer fatty and connective tissue. The FitzHugh-Nagumo model was used to simulate the propagation of the action potential from the SAN through the 3D right atrium model. The propagation sequence is shown in Fig. 1.

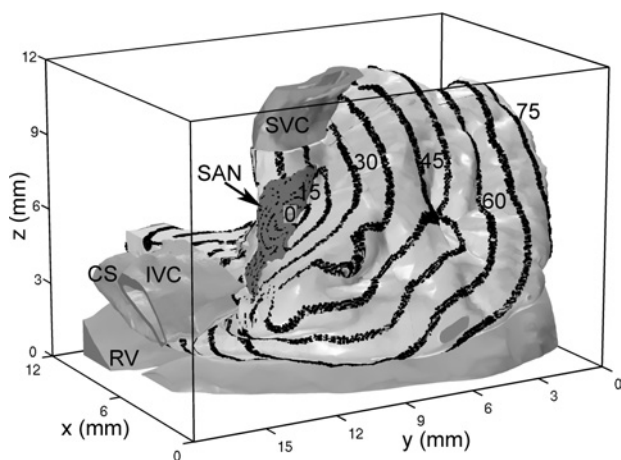


Figure 1. The propagation sequence of the action potential through the 3D right atrium. Isochrones are shown at 7.5 ms intervals.

Dobrzynski H et al. (2005). Circulation 111, 846-854.

Li J et al. (2004). Computers in Cardiology 31, 89-92.

Where applicable, the authors confirm that the experiments described here conform with The Physiological Society ethical requirements.

## PC32

### The role of transient outward potassium current in mammalian heart

L. Virag<sup>1</sup>, A. Kristof<sup>3</sup>, P.P. Kovacs<sup>1</sup>, Z. Horvath<sup>3</sup>, Z. Nagy<sup>1</sup>, C. Lengyel<sup>2</sup>, N. Jost<sup>3</sup>, J.G. Papp<sup>1,3</sup> and A. Varro<sup>1,3</sup>

<sup>1</sup>Department of Pharmacology and Pharmacotherapy, University of Szeged, Szeged, Hungary, <sup>2</sup>1st Department of Internal Medicine, University of Szeged, Szeged, Hungary and <sup>3</sup>Division of Cardiovascular Pharmacology, Hungarian Academy of Sciences, Szeged, Hungary

Previous studies suggested that transient outward potassium current (I<sub>to</sub>) plays an important role only during the early fast phase of repolarization, modulating the plateau phase potential, but its direct influence on the total repolarization is negligible. In this study we took advantage of the observation that at high (100  $\mu$ M) concentration chromanol 293B blocks not only the slow delayed rectifier (I<sub>Ks</sub>), but also largely inhibits I<sub>to</sub>. Therefore, in the presence of full I<sub>Ks</sub> block (by L-735,821) chromanol 293B induced change of action potential (AP) and of ionic currents can be attributed to its effect on I<sub>to</sub>. Based on this assumption, the aim of the present study was to investigate the role of I<sub>to</sub> in cardiac ventricular repolarization applying the standard micro-electrode and patch-clamp techniques.

Chromanol 293B (100  $\mu$ M), in the presence of full I<sub>Ks</sub> block (100nM L-735,821), lengthened the AP repolarization in both endocardial and epicardial dog right ventricular preparations. The next set of experiments was carried out in the presence of 100 nM dofetilide and 1  $\mu$ M BayK 8644 to impair the repolarization reserve of the preparations. In these measurements chromanol 293B excessively lengthened the AP compared to that found after application of another I<sub>Ks</sub> inhibitor, HMR-1556, which can be attributed to the I<sub>to</sub> blocking effect of chromanol 293B. In single dog ventricular myocytes the inactivation kinetics of I<sub>to</sub> current was biexponential (rapid phase:  $3.89 \pm 0.13$  ms, amplitude:  $2222 \pm 239$  pA; slow phase:  $23.5 \pm 2.5$  ms, amplitude:  $172 \pm 33$  pA; n=12, test potential: 20 mV, means  $\pm$  S.E.M.). The amplitude and the time constant of the slow phase of I<sub>to</sub> imply an important role of the slowly inactivating I<sub>to</sub> in the plateau phase of the action potential. The little overlap of the inactivation and activation curves over the potential range of 0 to -40 mV proposes that a small fraction of these ion channels may reactivate in this potential range (I<sub>to</sub> "window current"). The I<sub>to</sub> current during the AP plateau and repolarization phases was measured as chromanol 293B sensitive current in left ventricular myocytes isolated from dog hearts using an AP waveform for the command potential. It was found that I<sub>to</sub> carries significant outward current in the plateau and also in the later phase of repolarization of the AP.